Protein Partitioning in Two-Phase Aqueous Polymer Systems. 3. A Neutron Scattering Investigation of the Polymer Solution Structure and Protein–Polymer Interactions

Nicholas L. Abbott,† Daniel Blankschtein, and T. Alan Hatton*

Department of Chemical Engineering, Massachusetts Institute of Technology, Cambridge, Massachusetts 02139

Received December 31, 1991; Revised Manuscript Received April 27, 1992

ABSTRACT: The intensities of neutrons scattered at small angles (SANS) (0.03 Å^{-1} < q < 0.3 Å^{-1}, where q is the scattering vector) from aqueous (D_2O) solutions of poly(ethylene oxide) (PEO) were measured over a wide range of polymer concentrations (0.8% w/w to 25% w/w) and molecular weights (1500–860 000 Da). A transition was measured from the dilute to the entangled polymer solution regimes with increasing PEO molecular weight (at constant PEO weight fraction) or with increasing PEO weight fraction (at constant PEO molecular weight). In solutions containing approximately 10% w/w PEO, the transition was detected in the vicinity of PEO 10 000 Da, which supports our recently advanced hypothesis that changes in PEO molecular weight influence protein partitioning in the two-phase aqueous PEO–dextran system through an accompanying transition in the structure of the PEO-rich solution phase. To elucidate the roles of repulsive steric and attractive forces on the interactions of hydrophilic proteins and PEO, SANS measurements of (1) aqueous solutions of PEO 8650 Da containing identifiable PEO coils, (2) aqueous solutions of bovine serum albumin (BSA), and (3) aqueous solutions containing a mixture of BSA and PEO 8650 Da were performed. Although the net interaction between the 8650 Da PEO and BSA was found to be strongly repulsive, the second virial coefficient reflecting protein–polymer interactions was found to be only 80% of the value predicted for purely excluded-volume interactions, thus suggesting the existence of an attractive interaction between a PEO coil and BSA. A quantitative model of the solution structure indicates that an attractive interaction energy of about $0.05kT$ (per polymer segment interacting with the protein) is sufficient to describe the influence of BSA–PEO interactions on the SANS intensity measurements. This is consistent with recently developed *statistical-thermodynamic* models of protein–polymer interactions in the two-phase aqueous PEO–dextran system.

1. Introduction

Although the partitioning of proteins and other biological molecules in two-phase aqueous polymer systems has received considerable attention over the past 30 years through equilibrium experiments and thermodynamic theories, such as the measurement and prediction of protein partition coefficients, many aspects of the molecular-level mechanisms responsible for the observed phenomena are not yet fully understood.[1-7] In a recent series of papers,[8,9] hereafter referred to as papers 1 and 2, respectively, the nature of the interactions between the flexible and diffuse polymer molecules and the rigid and compact protein molecules were explored through the development of molecular-level pictures for polymer solution phases containing globular proteins. In the two-phase aqueous system containing poly(ethylene oxide) (PEO) and dextran, where an aqueous PEO-rich solution phase coexists with an aqueous dextran-rich solution phase, these physical pictures were based, in part, on a proposed transition in the nature of the PEO-rich phase from the dilute to the entangled polymer solution regimes with increasing PEO molecular weight.

Accompanying the development of the molecular-level pictures for the interactions between proteins and polymers in solution, complementary thermodynamic descriptions were advanced for each physical picture to predict the associated protein partitioning behaviors.[8] It was concluded that although the physical exclusion of the proteins by the polymers contributes to the observed partitioning behavior, other interactions between polymers and proteins need to be considered to explain the observed partitioning trends. In particular, the influence of the PEO molecular weight on the partitioning behavior of the series of proteins[10,11] cytochrome c, ovalbumin, bovine serum albumin, catalase, pullulanase, and phosphorylase was observed to be consistent with the presence of a weak attractive interaction (in addition to physical exclusion) between the protein molecules and the polymer coils.[8] Specifically, the experimental trends in the protein partitioning behavior were reproduced[9] by allowing for a weak attractive interaction energy, ϵ, which appeared to increase with protein size, R_p, where 19 Å < R_p < 52 Å, from order $0.01kT$ to $0.1kT$ per polymer segment at the protein surface, where k is the Boltzmann constant and T is the absolute temperature.

The aim of the work presented in this paper is to support and confront these recent theoretical developments on the partitioning of proteins in two-phase aqueous polymer systems through a comparison with more precise experiments. The experimental investigation reported in this paper, paper 3, represents a significant departure from the many previous experimental investigations[1-7] of protein partitioning in two-phase aqueous polymer systems in that we probe, using small-angle neutron scattering (SANS) techniques,[12-14] *both* the *structure* and the *thermodynamic properties* of aqueous polymer solution phases which contain proteins, rather than measuring only thermodynamic properties such as protein partition coefficients. We also deal with a one-phase system and, in so doing, remove the ambiguity associated with the interpretation of the protein partitioning behavior in two-phase aqueous polymer systems, where the experimental measurements reflect the *difference* between the interactions of proteins with each of the *two* coexisting polymer solution phases.

* To whom all correspondence should be addressed.
† Present address: Department of Chemistry, Harvard University, Cambridge, MA 02138.

0024-9297/92/2225-3932$03.00/0

The remainder of this paper is organized as follows. In section 2, experimental considerations associated with SANS from aqueous PEO solutions, aqueous bovine serum albumin (BSA) solutions, and their aqueous mixtures are discussed. Bovine serum albumin was chosen as a model hydrophilic protein because it has been the subject of prior SANS investigations,[15-17] and its partitioning behavior in two-phase aqueous polymer systems containing PEO-rich phases has also been examined.[11] In sections 3 and 4, the measurement and interpretation of SANS from (i) aqueous PEO solutions and (ii) aqueous BSA solutions, respectively, are presented. In particular, we reexamine the proposal advanced in paper 1 that the underlying influence of changes in PEO molecular weight on protein partitioning in the two-phase aqueous PEO–dextran system is a transition in the structure of the PEO-rich solution phase (as discussed above).[8]

In section 4, measurements presented for the neutron intensities scattered from BSA solutions (without PEO) serve two central purposes. First, the measurements confirm that the solutions are sufficiently dilute so that protein–protein interactions are not a dominating factor in determining the intensity of scattered neutrons. Second, the measurements enable the determination of the contrast factor of BSA in D_2O, which is a prerequisite for the interpretation of SANS from solutions containing mixtures of BSA and PEO.

In section 5, SANS measurements from mixtures of PEO and BSA in aqueous solution are presented. Interpretation of the scattering results provides the first independent experimental evidence that, while the net interaction between BSA and PEO is repulsive, the strength of this repulsive interaction is less than that corresponding to purely excluded-volume interactions. This is consistent with previous statistical–thermodynamic models[8,9,18-20] which suggest that a weak attractive interaction exists between the PEO coils and certain protein molecules, mediated by water, although the net interaction remains repulsive. A quantitative comparison is made between the strength of the attraction required to predict the SANS measurements from solutions containing BSA and PEO and that required to predict the partitioning behavior of BSA in two-phase aqueous PEO–dextran systems, and a good agreement is found. Finally, section 6 presents our concluding remarks.

2. Materials and Experimental Methods

A. Materials. Molecular weight standard grade PEO was purchased from Polysciences Inc. (Warrington, PA), having molecular weights (in Da) of 1450 (M_w/M_n = 1.10), 4250 (M_w/M_n = 1.10), 8650 (M_w/M_n = 1.10), and 23 000 (M_w/M_n = 1.13), and from Toyo Soda (Japan), having molecular weights of 45 000 (M_w/M_n = 1.07), 85 000 (M_w/M_n = 1.06), 160 000 (M_w/M_n = 1.07), 270 000 (M_w/M_n = 1.09), and 860 000 (M_w/M_n = 1.17), where M_w and M_n are the weight-average and number-average molecular weights, respectively. The polydispersivity indices (M_w/M_n) were reported by the manufacturers. BSA was purchased from Sigma Chemical (St. Louis, MO), Catalog No. A-7030. The D_2O was purchased from Aldrich Chemicals (Milwaukee, WI) and had a nominal purity of 99.8%. All other chemicals used were of analytical reagent grade.

B. Sample Preparation and Measurements. For the SANS measurements of the PEO solutions reported in section 3A, the solvent was pure D_2O. This contrasts to the SANS measurements of aqueous PEO solutions and aqueous BSA solutions, as well as aqueous BSA–PEO solutions, reported in sections 3B, 4, and 5, respectively, where all solutions were prepared with 0.5 M sodium acetate at pH 5.6 (the isoelectric pH of BSA is approximately 4.9).[21] The inclusion of 0.5 M anhydrous sodium acetate had a negligible contribution to the incoherent scattering of the solution due to the hydrogens on the acetate ion.[13] The 0.5 M sodium acetate was included in all the samples connected with the investigation of PEO–BSA interactions to ensure that any salt effects, for example, on the solvent quality for PEO,[22,23] were present throughout all the SANS measurements. All experimental measurements were performed at 25 °C in a thermostated cell holder and at ambient pressure.

The SANS experiments were conducted at the Brookhaven National Laboratory's High Flux Beam Reactor (HFBR) using the Department of Biology's low-angle spectrometer.[24] The average neutron wavelength was 4.9 Å, and the neutron flux was typically 3.5×10^6 neutrons/(cm^2 s). The liquid samples were housed in flat cylindrical cells made of quartz having a path length of 2 mm. The raw neutron scattering measurements were corrected for (i) background scattering, (ii) empty cell scattering, (iii) sample transmission, and (iv) variations in the efficiency of the detector elements according to the method of Chen and Bendedouch.[17]

3. Neutron Scattering from Aqueous PEO Solutions

A. Measurement of the Polymer Solution Structure. In view of the importance of the predicted transition in the structure of the top PEO-rich phase (from singly dispersed polymer coils to an entangled polymer web) of the two-phase aqueous PEO–dextran system,[8,9] the first objective of the neutron scattering investigation was to test experimentally the existence of such a transition over the range of PEO concentrations and molecular weights typically encountered in two-phase aqueous PEO–dextran systems.

In general, the intensity of neutrons scattered at a scattering vector q from a solution containing polymer (component 2), $I_2(q)$, can be interpreted using the expression[25,26]

$$\frac{I_2(0)}{I_2(q)} = (1 + \xi^2 q^2) \tag{1}$$

where the correlation length, ξ, may be interpreted as $R_g/3^{1/2}$, where R_g is the effective radius of gyration of the polymer, in the limit of vanishing polymer concentration (provided that $q < 3^{1/2}/R_g$), that is, for dilute polymer solutions, or as $0.35\xi_b$,[27] where ξ_b is the polymer mesh or blob size,[28] for entangled polymer solutions (provided that $q < 1/0.35\xi_b$). Following the determination of the polymer solution correlation lengths from the SANS measurements, the range of q values used was checked to ensure that the constraints outlined above were satisfied.

Before reporting the correlation lengths determined for the aqueous PEO solutions, the qualitative features of typical scattering intensity profiles will be discussed. For example, Figure 1 presents the intensity of neutrons scattered from an aqueous solution of PEO having a molecular weight of 21 000 Da as a function of the scattering vector, q, for four PEO solutions which differ in their PEO concentrations. In the low-q region ($q < 0.04$ Å^{-1}), the decrease in the intensity with increasing polymer concentration reflects the contribution of the steric (repulsive) interactions between polymer coils to the structure of the solution. The fact that polymer–polymer interactions influence the observed scattering to this extent suggests that the polymer concentrations (0.025, 0.083, 0.124, and 0.204, as volume fractions) are in the vicinity of the crossover concentration, c^*, for PEO 21 000 Da.[13] Note that c^* is a characteristic polymer concentration which reflects a region of polymer solution behavior where the extensive entanglement of polymer coils occurs with either increasing polymer concentration or molecular weight. For PEO 21 000 Da, c^* is in the vicinity of 0.05 (volume

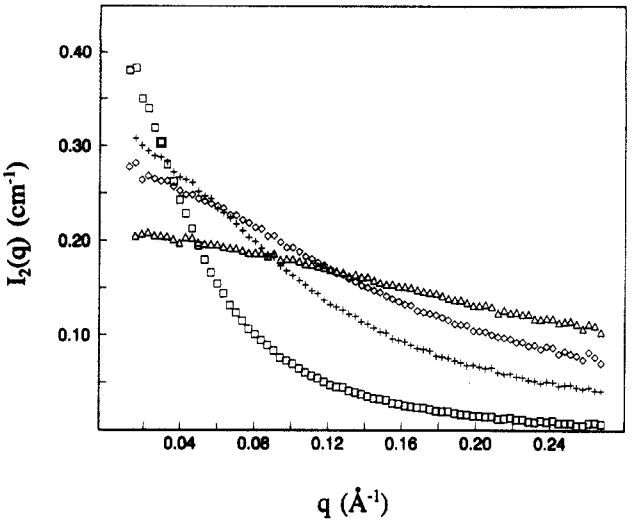

Figure 1. Measured neutron scattering intensity, $I_2(q)$, as a function of the magnitude of the scattering vector, q, for solutions of PEO 21 000 Da in D_2O. Polymer volume fractions: (□) 0.025; (+) 0.083; (◇) 0.124; (△) 0.204.

Table I
Polymer Solution Correlation Length, ξ, Deduced from SANS Measurements for Various Molecular Weights, M_2, and Volume Fractions, ϕ_2, of PEO in D_2O

M_2 (Da)	ϕ_2	ξ(Å)	M_2 (Da)	ϕ_2	ξ(Å)
860 000	0.008	45	9 000	0.058	10
	0.041	18		0.097	8.4
270 000	0.033	18		0.143	5.6
	0.067	12		0.167	4.6
160 000	0.054	13		0.250	2.8
	0.025	24	4 000	0.057	7.7
85 000	0.008	46		0.097	6.0
	0.047	15		0.140	5.3
	0.083	10		0.125	5.6
45 000	0.017	31		0.166	4.2
	0.083	10		0.250	2.5
	0.124	6.7	1 500	0.057	5.3
	0.039	16		0.097	4.6
21 000	0.025	23		0.140	3.9
	0.083	9.1		0.167	3.5
	0.124	6.3		0.250	2.5
	0.207	4.2			

fraction). In the high-q region ($q > 0.14$ Å^{-1}), where correlations between polymer segments over shorter length scales determine the scattered intensity (specifically, correlations within PEO coils), the magnitudes of the scattered neutron intensities rank in the opposite order with increasing polymer concentration. This follows from the fact that in the large-q limit, the nature of the correlations within each polymer coil is relatively insensitive to polymer concentration, and each polymer coil acts as an independent scatterer. Consequently, the scattered intensity is simply proportional to the polymer concentration. For the higher molecular weight polymers (not shown in Figure 1), the intersections of the scattered intensity curves with increasing concentration (which are shown in Figure 1 for PEO 21 000 Da) were either not observed, within the range of accessible scattering vectors, or were observed at very low q values. This observation reflects the fact that for the large polymer coils, over the accessible q range, only length scales smaller than the polymer coil size were probed, and therefore the measured intensity ranked in order of increasing polymer concentration.

Experimental measurements of the intensity of scattered neutrons as a function of q, analogous to those reported in Figure 1, were performed for the range of PEO molecular weights and volume fractions shown in Table I.

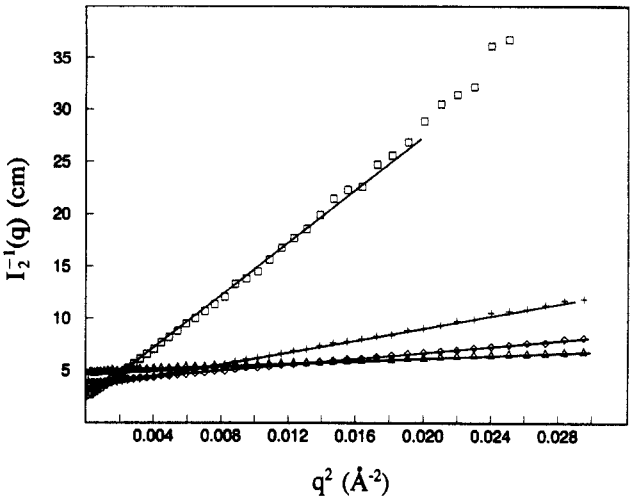

Figure 2. Reciprocal of the measured neutron scattering intensity, $I_2^{-1}(q)$, as a function of q^2, where q is the magnitude of the scattering vector, for solutions of PEO 21 000 Da in D_2O. Polymer volume fractions: (□) 0.025; (+) 0.083; (◇) 0.124; (△) 0.204.

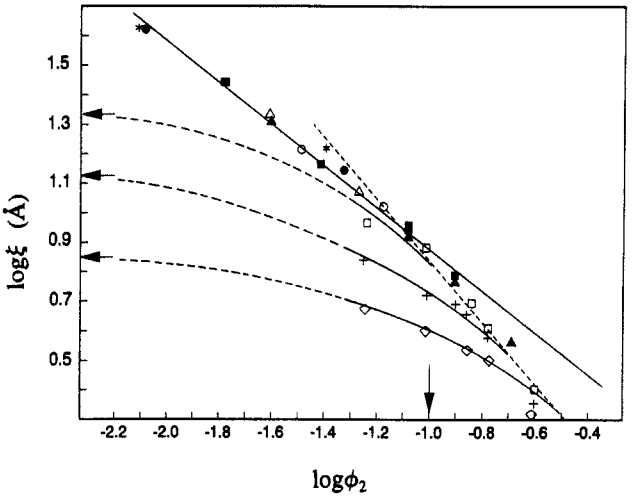

Figure 3. Logarithm of the static correlation length, log ξ, as a function of the logarithm of the PEO volume fraction, log ϕ_2, deduced from SANS measurements of PEO in D_2O. Polymer molecular weights (in Da): (*) 860 000; (○) 270 000, (△) 160 000; (●) 85 000; (■) 45 000; (▲) 21 000; (□) 9000; (+) 4000; (◇) 1500. See text in section 3 for an interpretation of the arrows and lines.

For all PEO solutions investigated, the scattered intensity was interpreted using eq 1 to yield a correlation length. For example, a plot of the data presented in Figure 1, in terms of the reciprocal intensity, $I_2^{-1}(q)$, as a function of q^2, as shown in Figure 2, yields the ordinate intercept as $I_2^{-1}(0)$, and the slope as $I_2^{-1}(0)\xi^2$. Accordingly, the correlation length ξ can be determined from the square root of the ratio of the slope and the ordinate intercept. Over the q^2 range 0.001–0.03 Å^{-2}, the plots presented in Figure 2 are essentially linear in accordance with the form suggested by eq 1. This procedure of determining ξ was repeated for all the other polymer molecular weights and volume fractions, and a summary of the deduced correlation lengths is presented in Table I. In Figure 3,the logarithm of the correlation lengths so determined is reported as a function of the logarithm of the PEO volume fractions for a range of polymer molecular weights between 1500 and 860 000 Da (data taken from Table I). Several regimes corresponding to different solution behavior can be identified. For the higher molecular weight polymers ($M_2 \gg$ 10 000 Da), the ξ values are observed to collapse onto a universal curve (solid line) over the range of polymer volume fractions reported in Table I. For these polymers,

the magnitude of ξ is independent of polymer molecular weight, being solely a function of the polymer volume fraction. This observation is consistent with the existence of an entangled polymer mesh within which the identities of the individual polymer coils are lost.[28] For polymers in good solvents and for probed length scales sufficiently large that excluded-volume interactions can swell the polymer coils locally, a simple scaling argument suggests that[28]

$$\xi \sim a\phi^{-3/4} \tag{2}$$

where ϕ is the volume fraction of polymer in solution and a is proportional to the size of a statistical polymer segment. In Figure 3, a full (straight) line having a slope of $-3/4$ has been passed through the experimental data points for the high molecular weight data. A close agreement between the slope of the data points and the theoretical prediction in eq 2 is apparent up to volume fractions of at least 0.10 ($\log \phi = -1$, as indicated by the vertical arrow).

In contrast to the universal behavior (molecular weight independence) observed for the high molecular weight polymers, the ξ values determined from the PEO samples having molecular weights of 1500, 4000, and 9000 Da were sensitive to the molecular weight of the polymer. The deduced ξ values were observed to increase with an increase in polymer molecular weight. This suggests that the structure of these solutions is sensitive to the sizes of the polymer coils and is therefore indicative of a polymer solution which contains identifiable polymer coils.[25,26] With decreasing polymer concentration, the ξ values for the low molecular weight polymers (1500, 4000, and 9000 Da) appear to be increasing toward a limiting value (dependent on the polymer molecular weight), which in the limit of vanishing polymer concentration should become equal to $R_g/3^{1/2}$ (according to eq 1). In Figure 3, on the ordinate axis, the correlation lengths evaluated according to $\xi = R_g/3^{1/2}$ are indicated by the horizontal arrows for PEO 1500, 4000, and 9000 Da, where R_g was determined from independent theoretical predictions.[9] The calculated ξ values (indicated by the horizontal arrows) appear to be consistent with an extrapolation of the measured values of ξ to vanishing polymer concentration. Clearly, additional measurements are required at lower polymer concentrations to make a more precise comparison. At a fixed volume fraction of low molecular weight PEO, for example, $\log \phi = -1$, the value of ξ was observed to increase with molecular weight but was always bounded by the ξ value of the solutions containing entangled high molecular weight PEO. The presence of the upper bound is consistent with the fact that, with increasing molecular weight, the polymer coils entangle into a mesh. Within the entangled polymer mesh, the identities of the individual polymer coils are lost and, therefore, the correlation length is observed to become independent of polymer molecular weight.[28] Finally, a more tentative observation can be made at high polymer concentrations where the correlation length values are small. In Figure 3, it appears that in the limit of high polymer concentrations (approximately greater than a volume fraction of 0.1 or $\log \phi = -1$, which is indicated by the vertical arrow), the correlation lengths display a universal behavior similar to that observed for the very high molecular weight polymer meshes, but with a higher value of the slope relating $\log \xi$ to $\log \phi$. The observed higher slope is consistent with the notion that at sufficiently small $\log \xi$ (or alternatively sufficiently large $\log \phi$), excluded-volume interactions between the polymer segments do not swell the local chain configuration significantly.[26,28] For this situation, a scaling argument similar to that used to obtain eq 2, but without excluded-volume effects, leads to[26,28]

$$\xi \sim a\phi^{-1} \tag{3}$$

The dashed (straight) line having a -1 slope which is plotted in Figure 3 appears consistent with the experimental deduction of ξ in the high-concentration region, although more experimental measurements are required to reach a definitive conclusion.

The central conclusion resulting from the experimental determination of the correlation lengths of aqueous PEO solutions is the confirmation of a transition in the polymer solution structure, from one containing identifiable polymer coils to one containing an entangled polymer mesh. In particular, at a PEO volume fraction of about 0.1, which is close to the concentration of PEO typically encountered in the PEO-rich phase of a two-phase aqueous PEO–dextran system, the onset of the molecular weight dependence of the correlation length occurs in the vicinity of a PEO molecular weight of about 10 000 Da. This is consistent with the previously reported[8] hypothesis of a transition in the PEO-rich phase structure on the basis of experimentally observed protein partitioning (a thermodynamic property). As stated earlier,[8] the transition in the solution structure is a gradual one, and in practice much of the protein partitioning occurs in the crossover region (with reference to Figure 3, the crossover for a particular PEO molecular weight can be defined as the range of polymer concentrations where the correlation length of the polymer solution is a function of both PEO molecular weight and volume fraction). This conclusion is not only relevant to past[8,9] and future theoretical developments but also impacts on our interpretation of the neutron scattering from polymer solutions containing proteins. That is, for the 5.9% w/w PEO solution of molecular weight 8650 Da (with BSA) that we investigate in detail in section 5, we have adopted an analysis which describes the interactions between identifiable polymer coils and protein molecules rather than an entangled polymer net interacting with protein molecules.

B. Neutron Scattering from Solutions of Identifiable PEO Coils. While in the previous section we reported polymer solution correlation lengths deduced from SANS measurements in order to identify the polymer solution regime, here we seek to provide an analysis of the scattering of neutrons from PEO solutions containing identifiable polymer coils which can be generalized to solutions containing mixtures of protein and PEO. We adopt the approach of Benoit and Benmouna,[29] in which the intramolecular and intermolecular correlations are predicted from the average configurations of the polymer coils in solution, which has been successful in describing the scattering from polymer solutions over a wide range of polymer concentrations.

We have examined the scattering of neutrons from a solution of 5.9% w/w PEO having a molecular weight of 8650 Da, since it is in this polymer solution that we have examined the excess scattering of neutrons in the presence of BSA. If we assume that the polymer coils are, on average, spherically symmetric, the scattered intensity of neutrons takes the following simple form[12-14]

$$I_2(q) = \frac{N_2}{V}\Delta\rho_2^2 (V_2^{\circ})^2 \langle P_2^2(q)\rangle S_2(q) \tag{4}$$

where N_2/V is the number density of polymer coils in solution, $\Delta\rho_2$ is the contrast factor (number of scattering sites per unit volume) between the polymer and the solvent, V_2° is the molecular volume of the polymer coil, $P_2(q)$ is

the form factor which reflects the intramolecular correlations between scattering sites within an individual polymer coil, $S_2(q)$ is the structure factor which reflects the contribution to the scattered intensity due to intermolecular correlations between scattering sites residing on different polymer coils, and the brackets, $\langle\ \rangle$, denote an averaging over all orientations of the polymer coil.

For a flexible polymer chain at Θ-solvent conditions, where the polymer chain statistics are Gaussian, the form factor is given by the well-known result first derived by Debye,[30,31] namely

$$P_2^2(x) = \frac{2}{x^2}(e^{-x} - 1 + x) \tag{5}$$

where $x = q^2R_g^2$. For polymers in good solvents, repulsive excluded-volume interactions between polymer segments within the same coil will cause chains of sufficient length to swell in size, and therefore, the chain statistics are no longer purely Gaussian.[32-35] Accordingly, for swollen polymers one can expect some deviation from eq 5. However, in the low-q region, specifically for $x < 10$, the deviation has been determined to be small.[32] Significantly, since $0 < x < 10$ corresponds to the important range of q values for the interpretation of the excess scattering from the mixture of PEO 8650 Da and BSA (see section 4), the approximation involved in using eq 5 does not limit our conclusions.

Benoit and Benmouna[29] generalized the classic Zimm model[36] for the small-angle scattering from dilute polymer solutions to that from solutions of arbitrary polymer concentration and obtained

$$S_2(q) = \frac{1}{1 + \nu(c)\rho_2 N^2 \langle P_2^2(c,q)\rangle} \tag{6}$$

where N is the number of polymer segments within a polymer coil, ρ_2 is the number density of polymer coils ($\rho_2 = N_2/V$), and the parameter $\nu(c)$, which characterizes the strength of the interactions between two polymer segments, is an effective parameter which reflects the contributions of multiple contacts between polymer chains and also depends on the polymer concentration, c. In view of the generalized definition of $\nu(c)$ and the difficulty associated with its a priori estimation,[37] we have determined its value by fitting eq 4 to the neutron scattering intensity measured from a solution of 5.9% w/w PEO having a molecular weight of 8650 Da. For the theoretical evaluation of $I_2(q)$ we have utilized eqs 5 and 6 in eq 4, along with the parameter values[9,13] $\rho_2 = 4.931 \times 10^{-6}$ Å^{-3}, $\Delta\rho_2 = 5.710 \times 10^{-6}$ Å^{-2}, $N = 197$, and $R_g = 36.5$ Å. In Figure 4, we show that a close agreement between the theoretically determined $I_2(q)$ values and the experimental values is obtained for $\nu(c = 5.9\%\ \text{w/w}) = 28$ Å^3. This deduced value of $\nu(c)$ appears consistent with the independent estimation[38] of $\nu(c) = 16$ Å^3 in the limit of vanishing PEO concentration in aqueous PEO solutions. At a higher polymer concentration, due to an increase in the number of multiple contacts between polymer coils, the value of $\nu(c)$ is expected to increase.[37] In general, the addition of salts (for example, 0.5 M sodium acetate, as used here) will influence the effective solvent quality for PEO and thus may also affect $\nu(c)$. Furthermore, the same change in solvent quality can be expected, in general, to influence the average configuration of the PEO coils, as described by R_g. However, using the value of $R_g = 36.5$ Å for PEO with a molecular weight of 8650 Da (determined in pure water and at a vanishing PEO concentration),[9] the measured intensity appears well predicted. This suggests that, in fact, the addition of 0.5 M sodium acetate does not greatly influence the average configuration adopted by the PEO molecules.

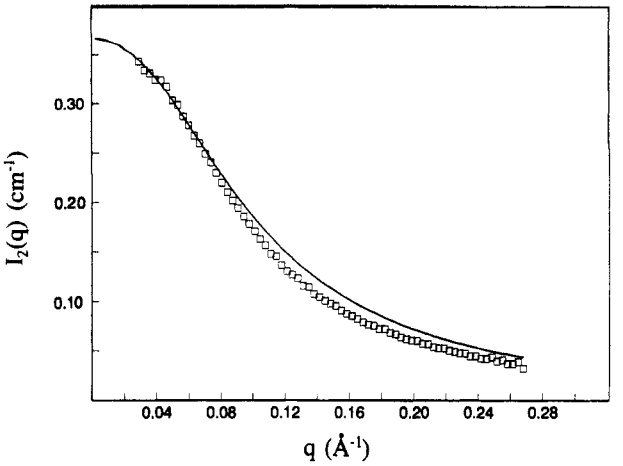

Figure 4. Neutron scattering intensity, $I_2(q)$, as a function of the magnitude of the scattering vector, q, for 5.9% PEO 8650 Da in D_2O: (□) experimental measurement, (—) theoretical prediction using the theory of Benoit and Benmouna.[32]

We have also evaluated the polymer solution structure factor, $S_2(q)$, using an approach that was motivated, in part, by the successful theoretical development reported[9] in paper 2 leading to the prediction of the vapor pressure of aqueous PEO solutions in the dilute solution regime. In this approach,[9] the polymer–polymer interaction was captured in terms of an effective hard-sphere potential, and an equation of state[39,40] for the resulting effective hard-sphere system was used to predict thermodynamic properties of the solution, such as the vapor pressure. Although a hard-sphere potential was used to describe the interactions between the PEO coils, the soft and penetrable nature of the coils was incorporated into the evaluation of their effective hard-sphere sizes.[9] In a similar spirit, we have evaluated $S_2(q)$ using a hard-sphere description[39] of the PEO solution and the previously developed hard-sphere potentials. Specifically, we calculated $S_2(q)$ from the direct correlation function, $C_2(q)$,[40] using the well-known Ornstein–Zernicke equation[41]

$$S_2(q) = \frac{1}{1 - \rho_2 C_2(q)} \tag{7}$$

The direct correlation function for a system of hard spheres has been evaluated previously[39] using the theory of Percus and Yevick[42] and is a function of η_2, the effective hard-sphere volume fraction of the polymer coils in the solution, which is given by

$$\eta_2 = \frac{\pi}{6}\rho_2 D_2^3 \tag{8}$$

where D_2 is the effective hard-sphere diameter of the polymer coils. For PEO having a molecular weight of 8650 Da in water and with a Flory–Huggins interaction parameter[43,44] $\chi = 0.45$, the radius of gyration, R_g, and effective hard-sphere radius, $D_2/2$, were predicted previously to be 36.5 and 22.4 Å, respectively.[9] In Figure 5, the predicted intensity of scattered neutrons (full line), $I_2(q)$ vs q, obtained using eqs 4, 5, 7, and 8, is compared to the experimentally measured intensity for the solution of 5.9% w/w PEO having a molecular weight of 8650 Da (data points). The *multiplicative* contributions of the form factor (dashed line) and the structure factor (dotted line) to the total intensity are also shown in Figure 5.

Inspection of Figure 5 leads to several observations. First, in the limit $q \to 0$, where the scattering reflects primarily the structure factor, $S_2(q)$, and thus the large-scale fluctuations in the system,[13] the magnitude of the

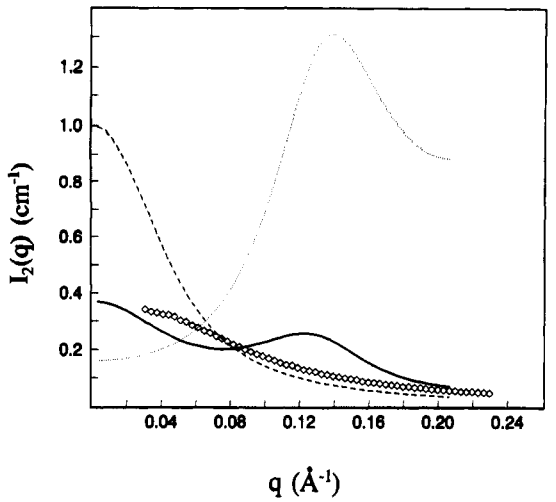

Figure 5. Neutron scattering intensity, $I_2(q)$, as a function of the magnitude of the scattering vector, q, for 5.9% PEO 8650 Da in D_2O: (◇) experimental measurement; (—) theoretical prediction using a hard-sphere structure factor, $S_2(q)$ (···); and theoretical prediction using a Debye form factor, $P_2(q)$ (- - -).

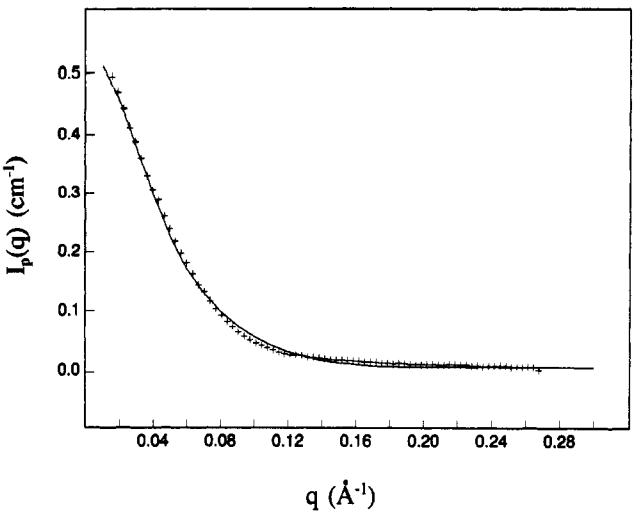

Figure 6. Neutron scattering intensity, $I_p(q)$, as a function of the magnitude of the scattering vector, q, for a solution of 9.9 g/L BSA in D_2O: (+) experimental measurement; (—) theoretical prediction using an ellipsoidal form factor and assuming a structure factor $S_p(q) = 1$.

predicted scattering intensity (full line) appears to agree with an extrapolation of the experimental measurements (data points). The scattering in this limit is essentially a measure of the thermodynamic state of the system (isothermal osmotic compressibility[38]), and therefore, the agreement between the measured and predicted intensity in the limit $q \to 0$ is consistent with the previously demonstrated ability of the effective hard-sphere model to predict thermodynamic properties, such as the vapor pressure, of aqueous PEO solutions.[9] This observation also supports our earlier assertion that the addition of 0.5 M sodium acetate does not greatly perturb the thermodynamic state of the aqueous PEO solution. It is also relevant to note that in the limit $q \to \infty$, where $S_2(q) \to 1$, the form factor of the PEO coils, $P_2(q)$, predicts the correct magnitude of the measured intensity of scattered neutrons. This observation supports our description of the PEO molecules as Gaussian coils.

In contrast to the close agreement between the predicted and measured neutron scattering intensities in both the low- and the high-q regions of Figure 5, at intermediate q values a significant oscillation is observed in the predicted neutron scattering intensity which is absent in the experimentally measured $I_2(q)$. This suggests that the prediction of the structural properties of the solution using an effective hard-sphere model is less successful than the prediction of thermodynamic properties. Presumably, this arises from the fact that the actual interactions between the PEO coils are somewhat softer and longer ranged than those accounted for by representing the polymer coils as effective hard spheres. Interestingly, the effective hard-sphere model appears quite successful in describing the excess scattering from solutions of protein and polymer (see section 5) suggesting, perhaps, that interactions between proteins and polymers are better modeled in terms of effective hard-sphere potentials than those between two polymer coils. This, in term, may relect the increased penetrability of a diffuse and flexible polymer coil toward another polymer coil, as compared to that toward a compact and impenetrable protein molecule.

4. Neutron Scattering from Aqueous BSA Solutions

Measurement of the neutron intensities scattered from aqueous bovine serum albumin (BSA) solutions (without PEO) served two central purposes. First, we confirmed that the protein solutions were sufficiently dilute so that protein–protein interactions had little effect (if any) on the intensity of scattered neutrons. Second, the contrast factor, $\Delta\rho_p$, for BSA in D_2O was determined. Both of these considerations are a prerequisite for the interpretation of neutron scattering from aqueous solutions containing PEO and BSA.

The intensity of neutrons scattered from aqueous BSA solutions was measured and interpreted using eq 4, where the subscript 2 (for the polymer) is now replaced by p to denote the protein. To simplify the interpretation of the BSA solution scattering, we have investigated solutions of BSA (in 0.5 M sodium acetate) which are sufficiently dilute for the protein molecules to be uncorrelated in their positions.[15] Accordingly, $S_p(q) = 1$, and the scattered intensity of neutrons should reflect solely the intramolecular correlations between scattering sites within individual BSA molecules. Under the condition of $S_p(q) = 1$, eq 4 simplifies to

$$I_p(q) = \frac{N_p}{V}\Delta\rho_p{}^2(V_p{}^o)^2\langle P_p{}^2(q)\rangle \qquad (9)$$

The shape of a BSA molecule is ellipsoidal,[15-17] and therefore the simple form factor for a sphere does not adequately describe the intensity of neutrons scattered from BSA solutions. In keeping with the previous neutron scattering investigations of BSA,[15-17] we have calculated the form factor of BSA as a prolate ellipsoid having dimensions 70 × 20 × 20 Å^3.

In Figure 6, the measured intensity of neutrons scattered from a 9.9 g/L BSA solution is compared to the theoretical evaluation using eq 9, where the contrast factor, $\Delta\rho_p$, was treated as a fitting parameter. For the calculation of the intensity of scattered neutrons, $I_p(q)$, reported in Figure 6, we have used $V_p = 117\,300$ Å^3,[15] and the number density of BSA molecules was calculated from the BSA concentration (9.9 g/L) as $N_p/V = 9.020\,83 \times 10^{-8}$ Å^{-3} using a BSA molecular weight of 66 700.[21] The best fit of the theoretical evaluation and the experimental intensity was obtained with $\Delta\rho_p = 2.1 \times 10^{-6}$ Å^{-2}, which is comparable to the value of 2.5×10^{-6} Å^{-2} obtained by Bendedouch and Chen.[15] The good agreement between the measured and calculated neutron scattering intensities supports the view of the protein as being ellipsoidal, as well as the assumption of $S_p(q) = 1$. The intensity of scattered neutrons was also calculated assuming spherical molecules with a volume

equivalent to that of the BSA molecule (not shown), and a significant deviation of the theoretical evaluation from the experimental data was evident.

5. Neutron Scattering from Aqueous Mixtures of PEO and BSA

Equation 4 can be generalized to describe the case of small-angle neutron scattering from a binary macromolecular mixture (PEO and BSA) in solution.[45] The general expression, simplified for the case where the protein is sufficiently dilute such that $S_p(q) = 1$ (see section 4 and below), is

$$I(q) = \frac{N_p}{V}\Delta\rho_p^2(V_p^\circ)^2\langle P_p^2(q)\rangle + 2\left(\frac{N_pN_2}{V^2}\right)^{1/2}\Delta\rho_p\Delta\rho_2V_p^\circ V_2^\circ\langle P_p(q)\rangle\langle P_2(q)\rangle S_{p2}(q) + \frac{N_2}{V}\Delta\rho_2^2(V_2^\circ)^2\langle P_2^2(q)\rangle S_2(q) \quad (10)$$

where $S_{p2}(q)$ is the partial structure factor which is of central interest to us since it contains the contribution of the interactions between the protein and the polymer molecules to the correlations within the solution that are reflected in the scattered intensity. Accordingly, it is useful to define the excess scattering of the mixture, $I^{ex}(q)$, by subtracting from the total intensity, $I(q)$, the intensity of neutrons scattered from aqueous solutions of protein (first term in eq 10) and polymer (third term in eq 10), separately. Subtracting these terms from eq 10 yields

$$I^{ex}(q) = 2\left(\frac{N_pN_2}{V^2}\right)^{1/2}\Delta\rho_p\Delta\rho_2\langle P_p(q)\rangle\langle P_2(q)\rangle S_{p2}(q) \quad (11)$$

It is important to qualify the conditions under which the subtraction leading to eq 11 is valid. Specifically, subtraction of the single-component scattering from the mixture is only valid under the conditions for which the form factors, $P_p(q)$ and $P_2(q)$, and the structure factors, $S_p(q)$ and $S_2(q)$, are the same in the mixture and the single-component solutions. Experimentally, this can be verified by measuring the excess scattered intensity of neutrons as a function of protein concentration. According to eq 11, if the subtraction is valid, the excess intensity, $I^{ex}(q)$, will be linearly proportional to the protein concentration ($S_{p2}(q)$ scales as $\rho_p^{1/2}$; see eq 13). This has been verified to be true for aqueous solutions of PEO and BSA up to 5 g/L BSA, at least, using light scattering measurements.[46] Furthermore, and as reported in section 4, the interpretation of the scattering of neutrons from a 9.9 g/L BSA solution (without polymer) was consistent with the fact that the interactions between BSA molecules make a negligible contribution to the overall scattered intensity of neutrons.

The measured excess scattered intensity from a solution containing 9.9 g/L BSA and 5.9% w/w PEO having a molecular weight of 8650 Da is reported in Figure 7 (data points). The excess scattering was measured to be negative over the entire range of q values (0.02–0.28 Å^{-1}). Qualitatively, this indicates that the *net* interaction between polymer coils and protein molecules in solution is repulsive.[13] In the limit $q \to 0$, the excess scattered intensity can be related to the concentration fluctuations in solution by[46]

$$I^{ex}(q\to 0) = K\left\langle\frac{\delta N_p\delta N_2}{V^2}\right\rangle \quad (12)$$

where $\delta N_i/V$ is the instantaneous fluctuation in the number density of molecules of type i (i = 2 or p) in solution and

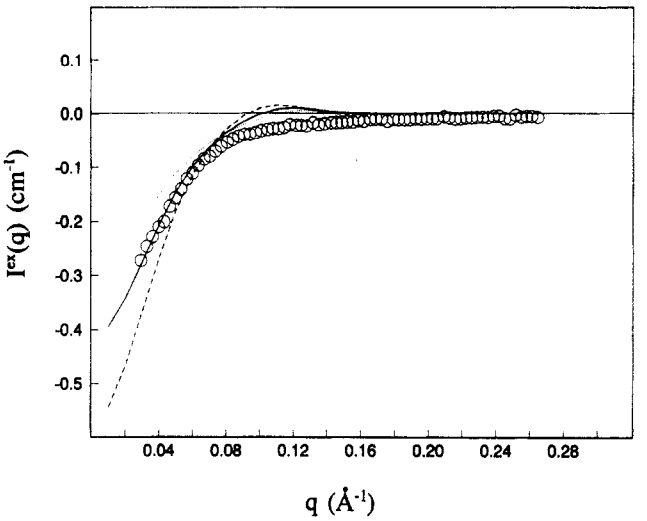

Figure 7. Excess neutron scattering intensity, $I^{ex}(q)$, as a function of q, the magnitude of the scattering vector, for a solution of 9.9 g/L BSA and 5.9% w/w PEO 8650 Da in D_2O: (O) experimental measurement, theoretical prediction using a hard-sphere mixture structure factor with three different protein sizes [(- - -) 34 Å, (—) 29 Å, (···) 24 Å].

K is a positive constant. When a net repulsion exists between the two species, on average, the two species will tend to reside apart from one another, and as is reflected in Figure 7, the right-hand side of eq 12 will be negative. Alternatively, for a net attraction between the molecules in solution the excess scattered intensity will be positive.[50]

In Figure 7, as the magnitude of the scattering vector increases, the excess scattering approaches zero asymptotically. This is because the scattering in the high-q region is dominated by intraparticle correlations which are essentially the same in both the mixture and the single-component solutions.[12-14]

The challenge in quantitatively predicting the excess scattered intensity, $I^{ex}(q)$, is in evaluating the partial structure factor $S_{p2}(q)$ (see eq 13), since all other quantities required to predict $I^{ex}(q)$ can be evaluated from the scattering measurements reported in sections 3 and 4. The partial structure factor, $S_{p2}(q)$, can be calculated using the Ornstein–Zernike equation[41] for a two-component hard-sphere system from the direct correlation functions, $C_{ij}(q)$.[41,47] This calculation is simplified since in section 4 it was demonstrated that the protein concentration is sufficiently low such that $S_p(q) = 1$. In that case one obtains

$$S_{p2}(q) = \frac{\rho_p^{1/2}\rho_2^{1/2}C_{p2}(q)}{1-\rho_2C_2(q)} \quad (13)$$

Furthermore, in the limit of vanishing protein concentration, the influence of the protein presence on the structure of the polymer solution will vanish, and therefore, $S_2(q)$ will be unchanged from the measurement and evaluation presented in section 3. To evaluate the direct correlation functions, $C_2(q)$ and $C_{p2}(q)$ appearing in eq 13, three approaches were explored (see below), each of which contained different approximations. Despite this, they all lead to the common conclusion suggesting the presence of attractive interactions between the protein molecules and the polymer coils (in addition to the steric repulsions).

In the first approach, the structure factors, $S_{p2}(q)$ and $S_2(q)$, were predicted from the direct correlation functions for a hard-sphere mixture, $C_{p2}(q)$ and $C_2(q)$, respectively, which have been derived previously by Lebowitz[47] using the Percus–Yevick equation[42] generalized for a multicom-

ponent system.[48,49] The inputs which are required to evaluate the direct correlation functions are the effective hard-sphere potentials of the polymer and the protein molecules. For PEO having a molecular weight of 8650 Da, the effective hard-sphere radius is 22.4 Å.[9] This is consistent with the hard-sphere potential used to predict the thermodynamic properties of aqueous PEO solutions in paper 2[9] and is also the potential used to predict the small-angle neutron scattering from PEO solutions in section 3. The effective hard-sphere protein radius was treated initially as a fitting parameter and subsequently compared with that evaluated using the Monte-Carlo method described in paper 2.[9] Note that the effective hard-sphere radius of the BSA molecule, when interacting with PEO, is not, in general, equal to the physical protein radius since the effective BSA hard-sphere radius reflects the deformable nature of the PEO coil.[9] In Figure 7 the experimental excess scattering is compared to the excess scattering predicted using the hard-sphere mixture structure factor for three different effective hard-sphere protein sizes of 34, 29, and 24 Å. The best agreement between the experimental data points and the theoretical prediction is obtained when a BSA radius of 29 Å is used. This value is significantly smaller than 37 Å, the value obtained for the effective hard-sphere radius of BSA assuming only steric interactions between BSA and the PEO molecules (see paper 2) using the Monte-Carlo method.[9] This observation is suggestive of an attractive interaction between the protein and the polymer molecules (in addition to the steric repulsion).[12-14] The influence of an attractive interaction between PEO and BSA would be to decrease the effective hard-sphere radius of a BSA molecule. Despite the weak attraction, the net interaction between the protein and the polymer molecules (which includes the contribution of steric interactions) remains repulsive, and thus the excess scattering intensity is negative.

In the second approach, the direct correlation function $C_{p2}(q)$ was also calculated from the Percus–Yevick equation for hard-sphere mixtures,[47] but in contrast to the first approach, the polymer structure factor, $S_2(q)$ (or alternatively $C_2(q)$), was evaluated using the previously described approach developed by Benoit and Benmouna.[29] This alternative description of the polymer solution was explored here because in section 3 it was shown that it leads to a better description of the polymer structure factor than does the hard-sphere model, particularly for intermediate q values. The effective hard-sphere polymer and protein radii used for the evaluation of $C_{p2}(q)$ were unchanged from the first approach. The result of this evaluation (not shown) was almost identical to the theoretical predictions presented in Figure 7. This suggests that the excess scattering intensity, $I^{ex}(q)$, is not very sensitive to the form of the PEO–PEO structure factor and, accordingly, that the correlations in the PEO coil positions (due to PEO–PEO coil interactions) do not have a dominating effect on the PEO–BSA correlations.

In the third approach, the excess scattering was predicted by explicitly introducing an attractive interaction between the protein and the polymer molecules, in addition to their steric repulsion. These two features, a repulsive core and an attractive part, are captured in the sticky hard-sphere potential model introduced by Baxter,[50] which has been applied successfully to the description of microemulsions[51,52] and other colloidal systems.[53] The model interaction potential for the case of a binary mixture (components n and m) is expressed in terms of τ_{nm}, the stickiness parameter[50] (which characterizes the strength of the attractive interaction between the polymer coils

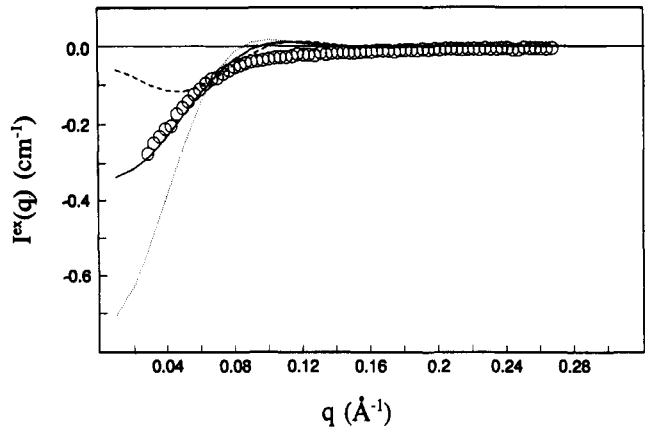

Figure 8. Excess neutron scattering intensity, $I^{ex}(q)$, as a function of q, the magnitude of the scattering vector, for a solution of 9.9 g/L BSA and 5.9% w/w PEO 8650 Da in D_2O: (○) experimental measurement, theoretical prediction using a sticky hard-sphere mixture structure factor with three different stickiness parameters, τ_{p2} [(---) 0.3, (—) 1.5, (···) ∞].

and the protein molecules, and where $\tau_{nm} = \infty$ corresponds to the hard-sphere limit, namely, no stickiness), and D_n and D_m are the hard-sphere diameters. For the case of a hard-sphere mixture with attractions between unlike species only, an analytical equation can be derived[54] for $C_{p2}(q)$ using the Percus–Yevick approximation.[42] The inputs to the evaluation of the sticky hard-sphere structure factor are the effective hard-sphere diameters of the proteins (D_p) and the polymers (D_2) and the stickiness parameter (τ_{p2}). As discussed above, the effective hard-sphere diameters which characterize the PEO–PEO coil interaction and the PEO–BSA steric interaction have been determined previously to be 44.8 and 74 Å, respectively.[9] In Figure 8, the excess scattering intensity measured experimentally is compared to the predicted intensity using the sticky hard-sphere structure factor for various values of the stickiness parameter, τ_{p2}. An inspection of Figure 8 reveals that in the absence of any attraction between the protein and the polymer molecules ($\tau_{p2} = \infty$), the predicted excess scattering is more negative than that observed experimentally in the low-q region. Furthermore, accompanying an increase in the strength of the attraction (a decrease in τ_{p2}), the predicted excess scattering intensity approaches that observed experimentally. A stickiness parameter of approximately $\tau_{p2} = 1.5$ was determined to produce the closest fit of the predicted excess scattering intensity to the experimental data.

Finally, it is relevant to discuss the "hump" that is present in the predicted excess scattering intensity at $q \simeq 0.1$ Å^{-1} in both Figures 7 and 8. In view of the earlier discussion of a similar hump in the predicted scattering of a PEO solution (see Figure 5), the most likely explanation lies in our characterization of the protein–polymer interaction using an effective hard-sphere model. In reality, the true interaction potential will be "softer" and longer ranged than the effective hard-sphere potential, and the effect of this "softness" will be to reduce the strength of the correlations within the solution, that is, to damp the oscillations in the structure factor. However, it is important to note that these considerations do not affect our conclusions in both the lower-q and higher-q regions, where good agreement is observed between the experimental and the theoretically predicted intensity.

To make a quantitative comparison between the strength of the attraction required to describe the neutron scattering data ($\tau_{p2} = 1.5$, in the notation of the sticky hard-sphere model[50]) and the strength of the attraction required in

paper 2 to account for the influence of PEO molecular weight on the protein partition coefficient (ϵ, in the notation of papers[8,9] 1 and 2), the second virial coefficient reflecting protein–polymer interactions[55] was calculated for both models. For the sticky hard-sphere model,[50] the second virial coefficient describing the protein–polymer interactions, B_{p2}, is related to the stickiness parameter and the hard-sphere diameters by[53]

$$B_{p2} = \frac{\pi}{6}\left(\frac{D_p + D_2}{2}\right)^3\left(4 - \frac{1}{\tau_{p2}}\right) \quad (14)$$

By substitution of sticky hard-sphere parameter values that describe the measured excess scattered intensity (determined above), that is, $\tau_{p2} = 1.5$, $D_2 = 44.8$ Å, and $D_p = 74$ Å, the second virial coefficient was evaluated from eq 14 to be 4.66×10^5 Å^3. Using the Monte-Carlo approach described in paper 2, the same value of the second virial coefficient is obtained with an attractive interaction energy of $\epsilon = 0.05kT$ (per polymer segment interacting with the protein surface). The strength of the attractive interaction energy, $\epsilon = 0.05kT$, predicted here from the measured intensity of neutrons scattered from an aqueous BSA–PEO solution, is consistent with previous values ($0.01kT$ to $0.10kT$) obtained on the basis of our earlier *thermodynamic* models for protein–polymer interactions,[8,9] which successfully predicted the partitioning behavior of proteins, such as BSA, in two-phase aqueous polymer systems containing PEO.

6. Concluding Remarks

We have reported experimental measurements of the intensity of neutrons scattered from solutions of PEO in D_2O over a wide range of PEO concentrations and molecular weights. The correlation lengths of the PEO solutions were determined from these experimental measurements, and a transition in the nature of the polymer solution phase was observed. That is, with an increase in PEO molecular weight, the PEO–D_2O system undergoes a transition from a polymer solution containing individually dispersed polymer coils to one containing an entangled mesh of polymers. Significantly, the PEO solution conditions at which the transition is observed correspond closely to those encountered in the PEO-rich phase of a two-phase aqueous PEO–dextran system utilized in protein partitioning experiments. In the spirit of the microscopic models of polymer solutions containing proteins proposed in two earlier papers of this series,[8,9] these experimental observations support our hypothesis that the underlying cause of a number of trends observed in protein partitioning measurements is the transition in the underlying polymer solution structure.[8] This recognition is fundamental for the development of physically based models of protein partitioning in two-phase aqueous polymer systems.

Neutron scattering measurements from solutions containing a mixture of PEO and BSA determined that the net interaction between the BSA and the PEO molecules is repulsive. Despite this net repulsive interaction, a simple model of the solution structure and the associated excess scattering suggests that the repulsive interaction is less than that expected on the basis of steric interactions alone. Accordingly, the existence of an attractive interaction between the protein and the polymer molecules is proposed on the basis of the predicted structure of the solution, as reflected in the SANS intensity measurements. This is consistent with previous statistical–thermodynamic models for the interactions of proteins and polymers which also suggested the presence of a weak attraction, in addition to the steric repulsion.[8,9,18-20] Quantitatively, both statistical–thermodynamic models and structural models for PEO solutions containing BSA predict that an attractive interaction of approximately $0.05kT$ (per polymer segment at the protein surface) exists between PEO and BSA. While clearly additional experiments with PEO over a range of molecular weights and concentrations, and with a variety of other proteins are required to solidify the propositions of this paper, the consistency between the microscopic models, statistical–thermodynamic theories, protein partitioning, and neutron scattering measurements is satisfying, and a unified description of interactions between certain types of proteins and polymers appears to be emerging.

Acknowledgment. Support for this work was provided by the National Science Foundation (NSF) through the Biotechnology Process Engineering Center at MIT under Grant CDR-88-03014 and a Presidential Young Investigator (PYI) Award to D.B. and by the Whitaker Foundation. In addition, D.B. was supported through an NSF Grant No. DMR-84-18718 administered by the Center for Materials Science and Engineering at MIT. D.B. is also grateful for the support by the Texaco-Mangelsdorf Career Development Professorship at MIT, as well as to BASF, British Petroleum America, Exxon, Kodak, and Unilever for providing PYI matching funds. N.L.A. is grateful to the George Murray Scholarship Fund of the University of Adelaide, Australia. Finally, we are very grateful for the friendly and helpful assistance of D. Schneider and S. H. Chen while performing the neutron scattering experiments at the Brookhaven National Laboratory, Brookhaven, NY.

References and Notes

(1) Albertsson, P. A. *Partition of Cell Particles and Macromolecules*; Wiley: New York, 1986.
(2) Walter, H., Brooks, D. E., Fisher, D., Eds. *Partitioning in Aqueous Two-Phase Systems*; Academic Press: New York, 1985.
(3) Walter, H.; Johansson, G. *Anal. Biochem.* **1986**, *155*, 215.
(4) Carlson, A. *Sep. Sci. Technol.* **1988**, *23*, 785.
(5) Baskir, J. N.; Hatton, T. A.; Suter, U. W. *Biotechnol. Bioeng.* **1989**, *34*, 541.
(6) Abbott, N. L.; Blankschtein, D.; Hatton, T. A. *Bioseparation* **1990**, *1*, 191.
(7) Walter, H.; Johansson, G.; Brooks, D. E. *Anal. Biochem.* **1991**, *197*, 1.
(8) Abbott, N. L.; Blankschtein, D.; Hatton, T. A. *Macromolecules* **1991**, *24*, 4334.
(9) Abbott, N. L.; Blankschtein, D.; Hatton, T. A. *Macromolecules*, preceding paper in this issue.
(10) Hustedt, H.; Kroner, K. H.; Stach, W.; Kula, M.-R. *Biotechnol. Bioeng.* **1978**, *20*, 1989.
(11) Albertsson, P.-A.; Cajarville, A.; Brooks, D. E.; Tjerneld, F. *Biochim. Biophys. Acta* **1987**, *926*, 87.
(12) Guinier, A.; Fournet, G. *Small Angle Scattering of X-Rays*; Wiley: New York, 1955.
(13) Cabane, B. In *Surfactant Science Series*; Zana, R., Ed.; Dekker: New York, 1987; Vol. 22.
(14) Glatter, O.; Kratky, O. *Small Angle X-Ray Scattering*; Academic Press; London, 1982.
(15) Bendedouch, D.; Chen, S.-H. *J. Phys. Chem.* **1983**, *87*, 1473.
(16) Nossal, R.; Glinka, C. J.; Chen, S.-H. *Biopolymers* **1986**, *25*, 1157.
(17) Chen, S.-H.; Bendedouch, D. *Methods Enzymol.* **1986**, *130*, 79.
(18) Baskir, J. N.; Hatton, T. A.; Suter, U. W. *Macromolecules* **1987**, *20*, 1300.
(19) Baskir, J. N.; Hatton, T. A.; Suter, U. W. *J. Phys. Chem.* **1989**, *93*, 2111.
(20) Forciniti, D.; Hall, C. K. *ACS Symp. Ser.* **1990**, *419*, 53.
(21) Squire, P. G.; Moser, P.; O'Konsky, C. T. *Biochemistry* **1968**, *7*, 4261.
(22) Ataman, M.; Boucher, E. A. *J. Polym. Sci., Polym. Phys. Ed.* **1982**, *20*, 1585.
(23) Florin, E.; Kjellander, R.; Eriksson, J. C. *J. Chem. Soc., Faraday Trans. 1* **1984**, *80*, 2889.

(24) Schneider, D. K.; Schoenborn, B. P. In *Neutrons in Biology*; Schoenborn, B. P., Ed.; Plenum: New York, 1984; p 119.
(25) Wiltzius, P.; Haller, H. R.; Cannell, D. S.; Schaefer, D. W. *Phys. Rev. Lett.* **1983**, *51*, 1183.
(26) Schaefer, D. *Polymer* **1984**, *25*, 387.
(27) Cabane, B.; Duplessix, R. *J. Phys.* **1987**, *48*, 651.
(28) de Gennes, P.-G. *Scaling Concepts in Polymer Physics*; Cornell University Press: Ithaca, NY, 1988.
(29) Benoit, H.; Benmouna, M. *Polymer* **1984**, *25*, 1059.
(30) Debye, P.; Bueche, A. M. *J. Appl. Phys.* **1949**, *20*, 518.
(31) Debye, P.; Henderson, H. R.; Brumberger, H. *J. Appl. Phys.* **1957**, *28*, 679.
(32) Tsunashima, Y.; Kurata, M. *J. Chem. Phys.* **1986**, *84*, 6432.
(33) Croxton, C. A. *Polym. Commun.* **1988**, *29*, 232.
(34) Boothroyd, A. T. *Polymer* **1988**, *29*, 1555.
(35) Bishop, M.; Saltiel, C. J. *J. Chem. Phys.* **1991**, *94*, 6920.
(36) Zimm, B. H. *J. Chem. Phys.* **1948**, *16*, 1093.
(37) Ullman, R.; Benoit, H.; King, J. S. *Macromolecules* **1986**, *19*, 183.
(38) Vennemann, N.; Lechner, M. D.; Oberthur, R. C. *Polymer* **1987**, *28*, 1939.
(39) Ashcroft, N. W.; Lekner, J. *Phys. Rev.* **1966**, *145*, 83.
(40) Hansen, J.-P.; McDonald, I. R. *Theory of Simple Liquids*; Academic Press: London, 1976.
(41) Ornstein, L. S.; Zernike, F. *Proc. K. Ned. Akad. Wet.* **1914**, *17*, 793.
(42) Percus, J. K.; Yevick, G. J. *Phys. Rev.* **1958**, *110*, 1.
(43) Flory, P. J. *Principles of Polymer Chemistry*; Cornell University Press: Ithaca, NY, and London, 1986.
(44) Huggins, M. L. *J. Chem. Phys.* **1941**, *9*, 440.
(45) Tong, P.; Witten, T. A.; Huang, J. S.; Fetters, L. J. *J. Phys. Fr.* **1990**, *51*, 2813.
(46) Knoll, D.; Hermans, J. *J. Biol. Chem.* **1983**, *258*, 5710.
(47) Lebowitz, J. L. *Phys. Rev.* **1964**, *133*, A895.
(48) Ashcroft, N. W.; Langreth, D. C. *Phys. Rev.* **1967**, *156*, 685.
(49) Ashcroft, N. W.; Langreth, D. C. *Phys. Rev.* **1968**, *166*, 934.
(50) Baxter, R. J. *J. Chem. Phys.* **1968**, *49*, 2770.
(51) Robertus, C.; Philipse, W. H.; Joosten, J. G. H.; Levine, Y. K. *J. Chem. Phys.* **1989**, *90*, 4482.
(52) Robertus, C.; Joosten, J. G. H.; Levine, Y. K. *J. Chem. Phys.* **1990**, *93*, 7293.
(53) de Kruif, C. G.; Rouw, P. W.; Briels, W. J.; Duits, M. H. G.; Vrij, A.; May, R. P. *Langmuir*, **1989**, *5*, 422.
(54) Barboy, B. *Chem. Phys.* **1975**, *11*, 357.
(55) McQuarrie, D. A. *Statistical Mechanics*; Harper and Row: New York, 1976.

Registry No. PEO, 25322-68-3.